

Global and regional changes in carbon dioxide emissions: 1970-2019

Nick James^a, Max Menzies^b

^a*School of Mathematics and Statistics, University of Melbourne, Victoria 3010, Australia*

^b*Beijing Institute of Mathematical Sciences and Applications, Tsinghua University, Beijing 101408, China*

Abstract

We introduce new frameworks to study spatio-temporal patterns in carbon dioxide emissions, demographic trends and economic patterns across 50 countries over the past 50 years. Our analysis is broken up into four sections. First, we introduce a new method to classify countries into one of three characteristic emissions classes based on a one, two or three-segment piecewise linear model. We reveal that most countries are best represented by a piecewise linear model with one change point. Next, we perform a decade-by-decade study of carbon dioxide trajectories. There, we demonstrate notable changes in cluster structures in each decade. We then study the spatial propagation of emissions over time, highlighting a peak in spatial dispersion in 2000, beyond which there has been a gradual decline in spatial emissions variance over space. Finally, we use carbon dioxide, GDP, and population data and apply dimensionality reduction and clustering to group countries based on similarity in their real and carbon economies.

Keywords: Carbon dioxide emissions, Time series analysis, Geographic variance, Dimensionality reduction, Clustering, Change point detection

1. Introduction

Currently, the greatest threat to our planet and the long-term prosperity of human life may be climate change. Climate change refers to long-term structural shifts in weather patterns and temperatures, largely driven by human activities such as the burning of fossil fuels and emission of carbon dioxide (CO₂). The long term effects of climate change include ocean warming, rising sea levels, and ice melt. Climatic changes have caused an estimated 150 000 deaths per year since 2002 [1], and the World Health Organization predicts that this level will rise to 250 000 deaths per year between 2030 and 2050 [2]. Thus, efforts by different governments to reduce CO₂ emissions are of the utmost importance

Email addresses: nick.james@unimelb.edu.au (Nick James),
max.menzies@alumni.harvard.edu (Max Menzies)

for mitigating this ongoing crisis. Mathematical analysis of CO₂ emissions over time may identify countries that have been particularly successful in reducing their emissions and provide exemplars for other countries.

Existing research on CO₂ emissions is broad, with diverse scientific focuses and methodologies. First, the underlying drivers of such emissions, often related to population dynamics, urbanisation and other societal factors has been covered broadly in the literature [3, 4, 5, 6, 7, 8, 9, 10, 11]. In particular, emissions are closely tied to economic growth, so their relationship has been studied closely [12, 13, 14, 15]. Numerous approaches have been taken to forecasting emissions [16, 17, 18, 19], including country-specific trends [20, 21] and offering solutions to the climate change crisis, such as carbon storage [22, 23]. Some papers have even studied spatio-temporal trends in CO₂ emissions [24, 25, 26]. Our paper takes a different approach, focusing on a thorough and descriptive analysis of trends in emissions on a country-by-country basis over the past 50 years. We focus our analysis on segmenting this entire window of analysis into smaller periods, revealing times of the greatest growth in emissions, the times of the largest geographic prevalence of emissions, and relationships with economic and population indices.

Our analysis relies on a broad existing literature of time series analysis as used by applied mathematicians and statisticians. Such methods have been applied widely within the physical and social sciences, including epidemiology [27, 28, 29, 30, 31, 32], finance [33, 34, 35, 36, 37, 38], and other fields [39, 40, 41, 42]. There are a variety of time series analysis frameworks that we draw upon, including parametric models [43, 44], techniques built upon distance metrics and similarity, [45, 46, 47, 48, 49], network analysis [50, 51, 52], clustering [53], and others [54, 55, 56, 57].

This paper proceeds as follows. In Section 2, we introduce a new method to identify characteristic emissions classes based on one of three piecewise linear models that best represents their emissions profile over the past 50 years. Next, Section 3 investigates this evolution more precisely, studying the collective similarity in emissions trajectories on a decade-by-decade basis between 1970 and 2019. We then explore the spatial propagation of emissions over time in Section 4, showing that CO₂ emissions around the world became more spatially disparate until 2000, followed by increased geographic concentration, primarily driven through China’s rapid growth. Finally, Section 5 compares different countries’ real and carbon economies via dimensionality reduction and clustering techniques. We conclude in Section 6.

2. Characteristic emissions classes

Throughout this paper, we use the $n = 50$ countries with the greatest total CO₂ emissions as of 2019. We list these alphabetically and index them $i = 1, \dots, n$. We study yearly data across $T = 50$ years, indexed $t = 1, \dots, 50$. Let $x_i(t) \in \mathbb{R}$ be the multivariate time series of the CO₂ emissions of country i in year t .

In this section, we introduce a new method to classify countries based on their emissions trends over time. Having noticed that many countries exhibit a

piecewise linear trend in their CO₂ emissions, we introduce a new framework to determine the most appropriate model for each country. We assume that each country's emission behaviours over time are well represented by one of the three following models:

1. Model 0 (M_0): a linear model with no change points.
2. Model 1 (M_1): a piecewise linear model with one change point (two piecewise linear components).
3. Model 2 (M_2): a piecewise linear model with two change points (three piecewise linear components).

In our algorithmic procedure, we select the optimal number and placement of up to two change points, such that the average R^2 of the various fits (one more than the number of change points) is maximised. Given a preference for a simpler model in the circumstance where a more complex one accounts for a similar level (or marginally more) explanatory variance, we introduce a slight penalty for model complexity. Specifically, suppose we have a single country's CO₂ emissions $x(t)$ over a period $t = 1, \dots, T$. We maximise the value of the average R^2 across piecewise linear models as follows:

$$\operatorname{argmax}_{0 \leq K \leq 2} \operatorname{argmax}_{1 = \xi_0 < \dots < \xi_{K+1} = T} \frac{1}{K} \sum_{i=0}^K R^2_{[\xi_i, \xi_{i+1}]} - \alpha K; \quad (1)$$

$$R^2_{[a,b]} = \max_{c,d} 1 - \frac{\sum_{t=a}^b (x(t) - (c + dt))^2}{\sum_{t=a}^b (x(t) - \bar{x})^2}. \quad (2)$$

In the equation above, $\alpha > 0$ is a penalty term, mildly penalising increasing the number of change points K (whereby the number of segments is $K + 1$). Having inspected the data, we impose a mild degree of regularisation, setting $\alpha = 0.01$. As the value of R^2 is commonly reported as a percentage, this penalty imposes just a 1% penalty on increasing the number of permissible segments.

We remark that the linear models above do not impose the assumption of continuity of the linear fits between segments. While this might seem surprising at first, we believe this is well supported by examining the eventual fits on the data, where clear discontinuities in emissions emerge. This is supported in the discussion of Figure 1 below.

We document the optimal model for each country in Table 1. There we see the most frequently occurring model is M_1 (with 23 countries), followed by M_2 (16 countries) and then M_0 (11 countries). That is, in the vast majority of cases, CO₂ emissions are best modelled by a piecewise linear model with two or three segments, indicating some heterogeneity over time in the growth rate of emissions.

In Figure 1, we display two representative countries for each model. In Figures 1a and 1b, respectively, we display trends for Algeria and Germany, revealing one persistent linear trend over the past 50 years. Algeria exhibits

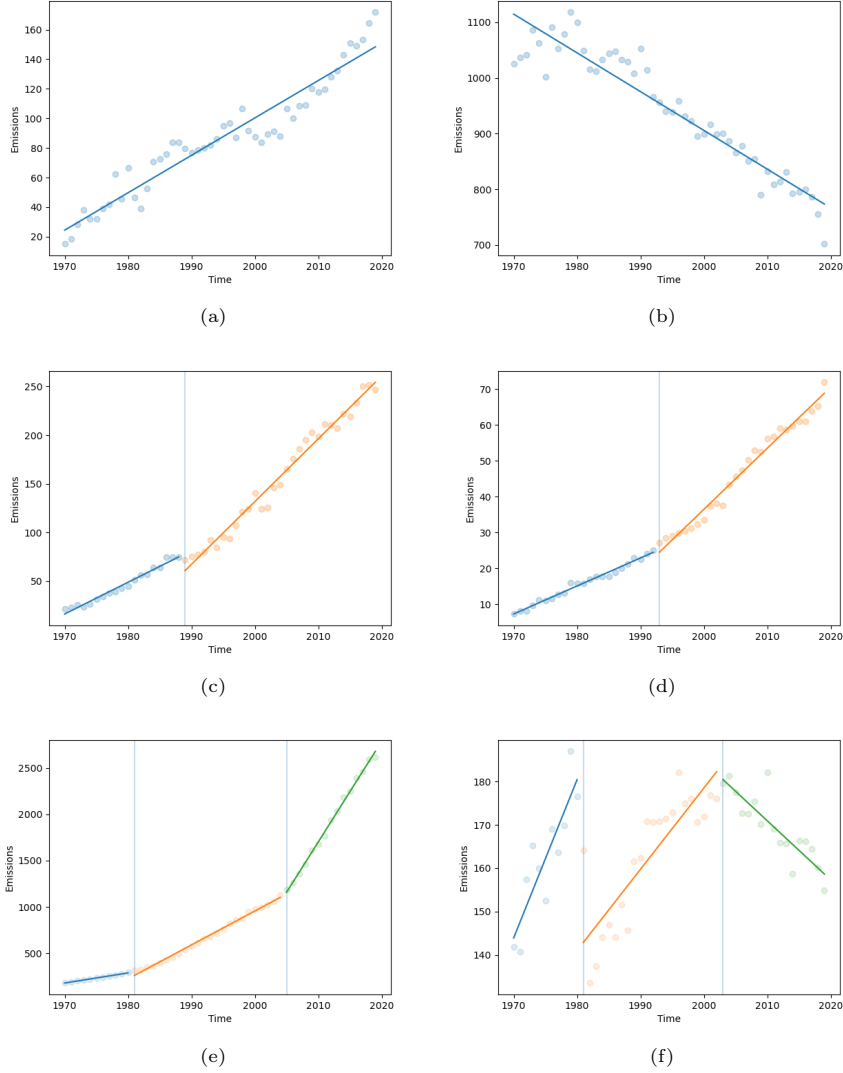


Figure 1: Country emissions (in billions of metric tonnes) and optimal piecewise linear fits. We provide two examples from each representative model. (a) Algeria and (b) Germany are best represented by model M_0 , (c) Egypt and (d) Morocco by model M_1 , and (e) India and (f) the Netherlands by model M_2 .

Country	Best model	Country	Best model
Algeria	M_0	Morocco	M_1
Argentina	M_1	Netherlands	M_2
Australia	M_0	Nigeria	M_1
Austria	M_2	Oman	M_1
Bangladesh	M_1	Pakistan	M_1
Belgium	M_2	Phillippines	M_1
Brazil	M_1	Poland	M_2
Canada	M_0	Qatar	M_1
Chile	M_0	Romania	M_1
China	M_2	Russia	M_2
Colombia	M_1	Saudi Arabia	M_1
Czechia	M_1	South Africa	M_0
Egypt	M_1	South Korea	M_0
France	M_2	Spain	M_2
Germany	M_0	Taiwan	M_0
India	M_2	Thailand	M_0
Indonesia	M_1	Turkey	M_0
Iran	M_1	Turkmenistan	M_2
Iraq	M_1	Ukraine	M_2
Italy	M_2	United Arab Emirates	M_1
Japan	M_1	United Kingdom	M_2
Kazakhstan	M_2	United States	M_1
Kuwait	M_0	Uzbekistan	M_2
Malaysia	M_1	Venezuela	M_1
Mexico	M_1	Vietnam	M_2

Table 1: Country and optimal piecewise linear models, defined in Section 2. The optimal model (and placement of change points) is determined by optimising a penalised averaged R^2 as in Eq. (1).

consistently increasing emissions, while Germany exhibits linearly decreasing emissions over the past 50 years. Egypt (Figure 1c) and Morocco (Figure 1d) both exhibit a more strongly positive linear increase beyond the late 1980s and early 1990s respectively. Fittingly, these countries are best modelled by one change point. Both India and the Netherlands, Figures 1e and 1f, respectively, require two change points (three segments) to best model their dynamics, fitting the numerous changes in their emissions' evolution over time. India exhibits clear continuity and increases in its emissions over time, which are appropriately captured by the adjoined linear fits. On the other hand, the Netherlands features clear discontinuities and abrupt changes in total emissions, seen in the early 1980s and early 2000s, respectively.

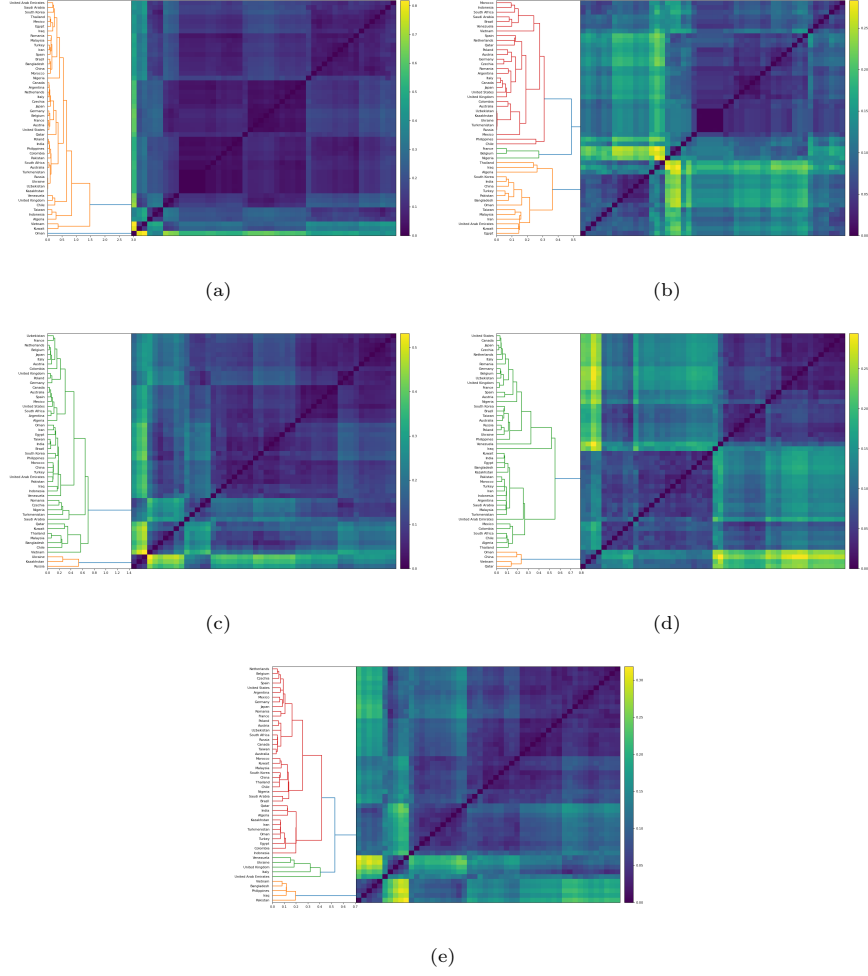


Figure 2: Hierarchical clustering applied to normalised CO₂ emissions trajectories on a decade-by-decade basis. (a) 1970-1979, (b) 1980-1989, (c) 1990-1999, (d) 2000-2009, (e) 2010-2019.

3. Emissions temporal partition analysis

In this section, we partition country emissions by decade and investigate on a decade-by-decade basis, exploring the evolutionary structure of country behaviours. We restrict each country's emission values to a particular decade, giving a sequence $\mathbf{f}_i = (f_i(1), f_i(2), \dots, f_i(m)) \in \mathbb{R}^m$, where $m = 10$ is the number of years in that decade, and $i = 1, \dots, n$ represent country index. Let $\|\mathbf{f}_i\| = \sum_{t=1}^m |f_i(t)|$ be the L^1 norm of the vector \mathbf{f}_i . As all $f_i(t)$ are non-negative, this counts the total emissions observed in a decade. We may then define $\mathbf{g}_i = \frac{\mathbf{f}_i}{\|\mathbf{f}_i\|}$. The vectors \mathbf{g}_i reflect relative changes in emissions within a decade. For example, a country whose emissions in a decade differ between 1000 and 1100 units (of mass) will present a relatively flat normalised trajectory, whereas a country whose emissions in a decade rise from 0 to 100 units will present a more steeply increasing normalised trajectory, as a reflection of the relative change. We define *trajectory distance matrices* $D_{ij} = \|\mathbf{g}_i - \mathbf{g}_j\|$ that measure distance between these normalised trajectories.

In Figures 2a, 2b, 2c, 2d and 2e, we implement hierarchical clustering on these matrices for the ten-year periods of 1970-1979, 1980-1989, up to 2010-2019. Both the number of clusters and cluster constituents are dynamic, with both varying as we proceed forward in time.

First, during 1970-1979, we observe a predominant cluster, consisting of three subclusters, and a small collection of outlier countries (primarily displayed as separate subclusters within the predominant cluster). All subclusters within the predominant cluster exhibit increasing trends of CO₂ emissions over the decade. The first subcluster consists of countries such as Russia (Figure 3a) and Ukraine - these countries are characterised by huge growth and accelerating emissions trends. The second subcluster, consisting of Italy, Canada and Argentina, exhibits moderate growth in CO₂ emissions. The final cluster, which includes Spain and Brazil, also displays relatively steady growth behaviours. The outlier countries, such as Vietnam and Kuwait, exhibit declining CO₂ emissions, which are anomalous with respect to the rest of the collection.

Next, we turn to the period 1980-1989. This period produces a dendrogram consisting of three distinct clusters. The first cluster contains countries such as India (3b) and China (3c), which display continued growth throughout the period. The second cluster consists of various countries, but displays pronounced similarity between Eastern Europe and Central Asia, countries such as Kazakhstan, Russia and Ukraine. These countries all experienced huge growth in emissions, peaking around 1990. The final cluster consists of France, Belgium and Nigeria. These countries display erratic emissions behaviours, with all trajectories displaying limited trend and substantial volatility.

In the 1990-1999 period, countries form one primary cluster, with a small collection of outlier countries in a separate, significantly smaller cluster. The primary cluster consists of countries that displayed consistent growth over the prior decade (to varying extents). The outlier cluster consists of countries such as Ukraine, Russia and Kazakhstan - these all experienced precipitous drops in their emissions at the beginning of the period, and continuing decline throughout

the decade.

The 2000-2009 period produces one primary trajectory cluster (consisting of two similarly sized subclusters) and a collection of outlier countries. The clear bifurcation in the large cluster is indicative of contrasting trends in emissions behaviours between various countries. The first subcluster consists of countries such as the Netherlands, Italy, Germany, the United States (Figure 3d), Canada, Japan (3e) and Belgium. Most countries within this subcluster are more developed and have taken a stronger stance in introducing policies to reduce emissions. Such countries exhibit either flat or declining emissions trajectories throughout the decade. The second subcluster, consisting of countries such as India (3b), Iran and Turkey, features sustained growth in emissions during this period. The significantly smaller second cluster consists of countries whose emissions profiles more resemble those of the second subcluster. This cluster consists of China (3c), Oman, Vietnam and Qatar.

Finally, we turn to the most recent decade of analysis, 2010-2019. This period produces three characteristic classes of emissions trajectories. The first cluster consists of countries with lower human development index (HDI) levels: Vietnam, Bangladesh, the Philippines, Iraq and Pakistan. These countries produce emissions trajectories that increase significantly throughout the period. The second cluster consists of Venezuela, Ukraine, the United Kingdom (UK), Italy and the United Arab Emirates (UAE). These countries mostly produce declining trajectories, which may signify their greater collective focus on reducing CO₂ emissions at the national level. The final cluster consists of two primary subclusters. The first contains countries such as Japan (3e), the Netherlands and Belgium. These countries are primarily characterised by erratic emissions output, with a declining trend overall. The second subcluster consists of countries such as China (3c), Thailand and Chile. Although these countries produce a positive trend over the entire decade, the rate of increase has slowed, and in some cases, overall emissions have begun to trend downward.

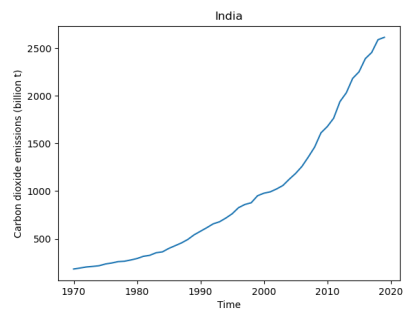
4. Evolutionary spatial emissions variance

In this section, we explore the evolution in geographic dispersion among our 50 countries' CO₂ emissions throughout our window of analysis. We study the multivariate time series $x_i(t)$ as a whole with a focus on the changing geographic spread of emissions over time. To do so, we convert each year's emissions values into a probability density function and incorporate real-world distances between countries to produce a measure of the physical spread of emissions across the world. Let $f(t) \in \mathbb{R}^n$ be the probability vector of CO₂ emissions produced by each country annually, divided by the total amount of emissions produced by our 50 countries that year. Specifically, let

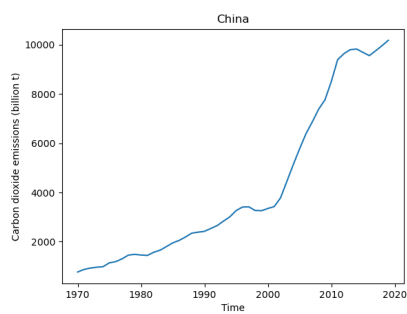
$$f_i(t) = \frac{x_i(t)}{\sum_{j=1}^n x_j(t)}, i = 1, \dots, n. \quad (3)$$



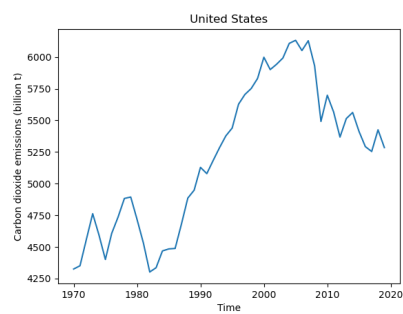
(a)



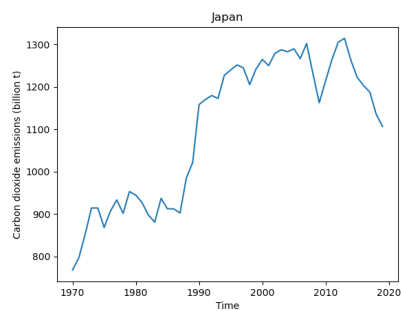
(b)



(c)



(d)



(e)

Figure 3: Country emissions (in billions of metric tonnes) over time for (a) Russia (b) India (c) China (d) the United States (e) Japan.

This produces a probability vector $f(t) \in \mathbb{R}^n$ for each year $t = 1, \dots, T$. We wish to use these probability distributions together with real-world distances to produce a time-varying measure of global dispersion of emissions. For this purpose, we apply the concept of geodesic variance introduced in [58] - this determines the total spread of a probability density function across any candidate metric space. Specifically, given a probability distribution f that corresponds to a measure μ sitting on a metric space (X, d) , we let

$$\text{Var}(f) = \int_{X \times X} d(x, y)^2 d\mu(x) d\mu(y) \quad (4)$$

$$= \sum_{x, y \in X} d(x, y)^2 f(x) f(y). \quad (5)$$

The second equality is valid when the metric space (X, d) is discrete, as is the case in our analysis. Henceforth, we apply this quantity in the instance where X is the set of 50 countries under consideration and $d(i, j)$ is the real-world haversine [59] distance between (the centroids of) any two countries indexed by i and j . We refer to (4) as the *geographic variance* of the probability distribution f ; it is computed as follows:

$$\text{Var}(f) = \sum_{i, j=1}^n d(i, j)^2 f_i f_j. \quad (6)$$

In Appendix A, we explain why we refer to this quantity with the word “variance”; we include a proof that it generalises the classical notion of the variance of a random variable on the real numbers \mathbb{R} .

In Figure 4, we plot the geographic variance $\text{Var}(f(t))$ of CO₂ emission distributions over time. The plot reveals several interesting findings. First, the trajectory features a broadly quadratic shape with a steady increase in emissions’ geographic variance until the year 2000, after which there is a steady decrease in variance. This shape is consistent with the theme that until the year 2000, globalisation and accompanying economic growth led to the propagation of CO₂ emissions all around the world, increasing geographic dispersion. The fall in this variance since 2000 indicates that the most serious emissions violators are becoming more spatially concentrated. We further investigate this evolution by studying the proportion of emissions by the three largest countries (by population and emissions): China, India and the United States (US). In 1970, the US was a clear leader in emissions, accounting for 32.7% of the distribution (across our 50 countries). By contrast, India and China only accounted for 7.8% and 5.8% of the distribution, respectively. In the year 2000, the US’ share of the total emissions distribution fell to 26.4%, with China’s contribution to the distribution increasing to 14.8% and India’s contribution falling to 4.3%. In the following 19 years, country emissions’ behaviours changed considerably. By 2019, China, the US and India account for 30.7%, 15.9% and 7.9% of the top 50 countries’ total emissions, respectively. These figures provide some insight into the overall

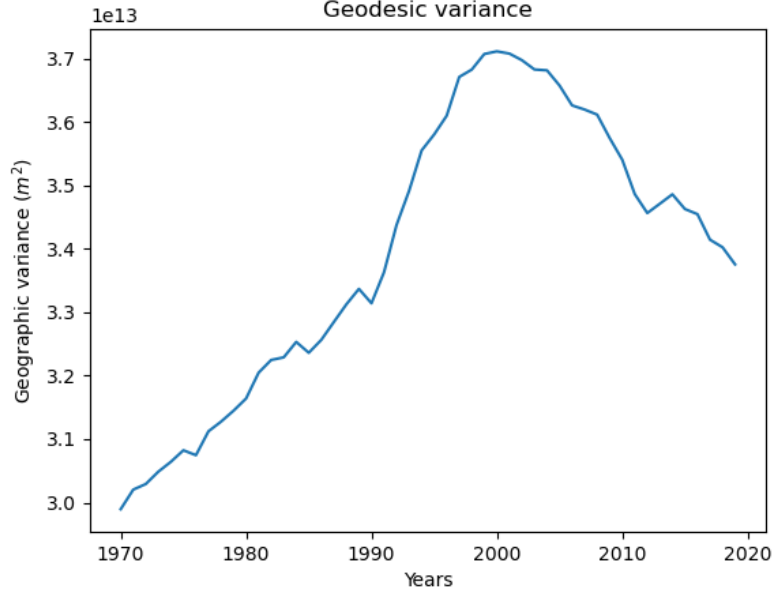


Figure 4: Geographic variance (in m^2) in carbon dioxide emissions between 1970-2019. The trajectory displays a noteworthy quadratic shape. Geographic variance in CO_2 emissions increase until 2000, beyond which they steadily decrease. This suggests that since 2000 there is less spatial dispersion in the bulk of CO_2 emissions.

shape displayed in Figure 4. In particular, the reduction in geographic variance exhibited since 2000 could be symptomatic of rapid growth in CO_2 emissions produced by China, causing a reallocation of the country’s contribution to the overall emissions total, consistent with a larger proportion of emissions coming from a more spatially concentrated area.

5. Relationships between the real and carbon economies

In this section, we investigate countries that share similar economic, demographic and emissions histories. First, we gather GDP, population and CO_2 emissions data over the past 50 years and generate distance matrices between all countries for each respective metric. Next, we generate an aggregate distance matrix, appropriately normalising for each quantity therein. We then apply multidimensional scaling (MDS) to the distance matrix, projecting the matrix into a lower-dimensional vector space, and then apply K-means clustering to the resulting projection. The number of clusters k is determined by optimising the silhouette score [60]. For the sake of interpretability, we accompany these K-means clustering results with a hierarchical clustering dendrogram.

Specifically, we form our normalised aggregate distance matrix by considering the multivariate time series of gross domestic product (GDP) and population

data $y_i(t)$ and $z_i(t)$, respectively, in addition to the aforementioned emissions data $x_i(t)$. We define $n \times n$ distance matrices as follows:

$$D_{ij}^X = \sum_{t=1}^T |x_i(t) - x_j(t)|; \quad (7)$$

$$D_{ij}^Y = \sum_{t=1}^T |y_i(t) - y_j(t)|; \quad (8)$$

$$D_{ij}^Z = \sum_{t=1}^T |z_i(t) - z_j(t)|. \quad (9)$$

For each matrix D , let $\|D\|_\infty$ be the maximal element of D . Our normalised aggregated matrix is then formed as follows:

$$\Omega = \frac{1}{\|D^X\|_\infty} D^X + \frac{1}{\|D^Y\|_\infty} D^Y + \frac{1}{\|D^Z\|_\infty} D^Z. \quad (10)$$

We then apply multidimensional scaling to this matrix to find point projections in 3D space. This procedure selects $z_1, \dots, z_n \in \mathbb{R}^3$ to minimise the following discrepancy score:

$$\sum_{i,j=1}^n (\Omega_{ij} - \|z_i - z_j\|)^2. \quad (11)$$

This is a necessary preprocessing step before K-means clustering can be applied. We choose three-dimensional projections as the matrix Ω is approximately a distance matrix between three-dimensional vectors. Indeed, suppose for two countries i, j we have uniformly for all time, $x_i(t) > x_j(t)$, $y_i(t) > y_j(t)$ and $z_i(t) > z_j(t)$. This is typically seen when a country indexed i is consistently larger than one indexed j . Then Ω_{ij} simplifies to

$$\Omega_{ij} = \omega_i - \omega_j, \quad (12)$$

$$\omega_i = \frac{1}{\|D^X\|_\infty} \sum_{t=1}^T x_i(t) + \frac{1}{\|D^Y\|_\infty} \sum_{t=1}^T y_i(t) + \frac{1}{\|D^Z\|_\infty} \sum_{t=1}^T z_i(t). \quad (13)$$

Thus, for many pairs of countries i, j , the distance Ω_{ij} can be expressed as a L^1 distance between three scalars, which approximates a Euclidean distance in \mathbb{R}^3 .

When we apply this analysis to all 50 countries, the US exhibits highly anomalous behaviour. In fact, we must sequentially remove the US, China, India, Russia and Japan (some of the largest countries with respect to emissions) to identify the general structures without these outlier countries. In the proceeding analysis, we remove these five countries, and study the structural patterns among the remaining countries.

First, we explore the similarity between countries with respect to each metric

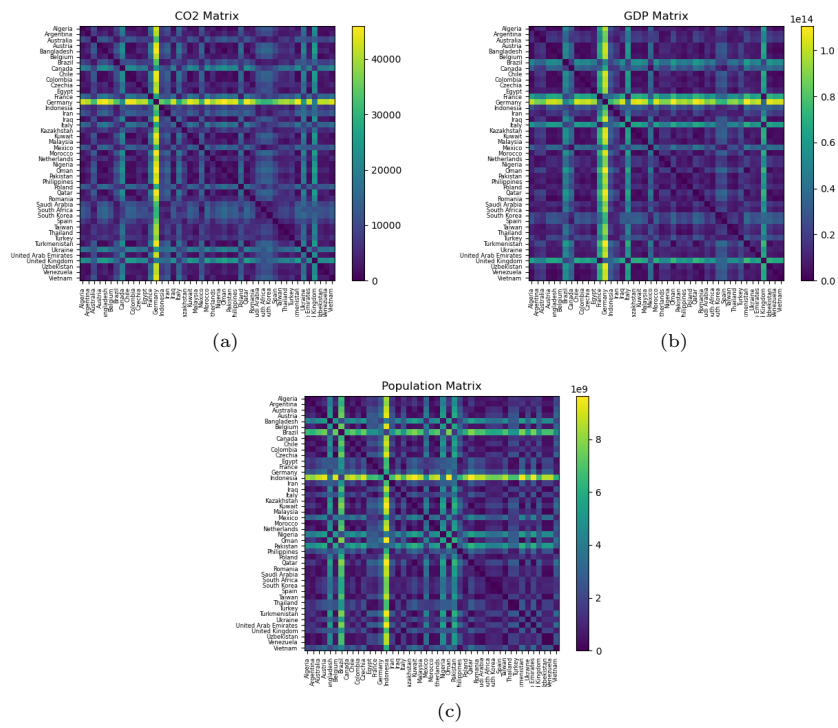


Figure 5: Distance matrices between (a) CO₂ emissions, defined in (7), (b) GDP, defined in (8), (c) population, defined in (9).

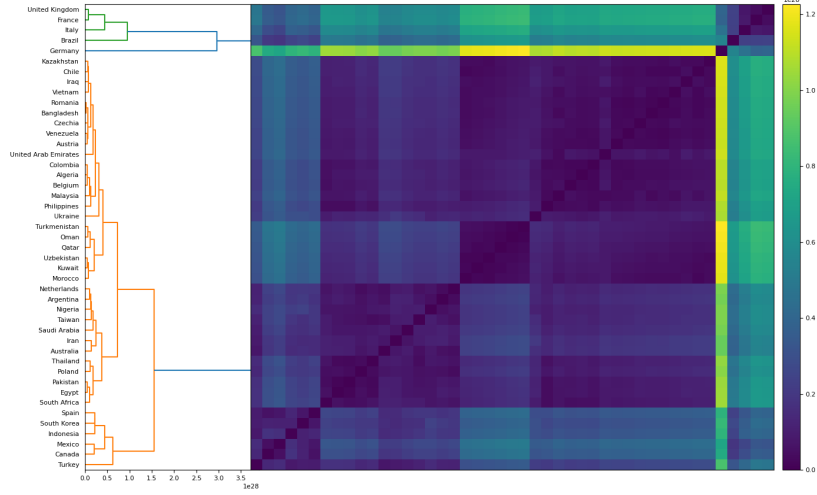


Figure 6: Hierarchical clustering applied to our aggregate normalised distance matrix Ω , which captures similarity in historical trends between countries’ real and carbon economies.

individually. Figure 5 displays the three distance matrices for CO_2 emissions, GDP, and population. In Figure 5a, Germany exhibits the greatest dissimilarity to the remainder of the collection of countries. Indeed, as seen in Figure 1b, Germany exhibits consistently decreasing emissions over time, unlike almost any other country. In Figure 5b, one can see that Germany, France and the UK are the most anomalous countries with respect to GDP based on their significant economic output over the past 50 years. In Figure 5c, we see the distance between country populations, where Indonesia, Brazil and Bangladesh exhibit the greatest dissimilarity to the rest of the collection.

Next, we turn to the aggregated distance matrix, which intends to uncover countries that are similar both in terms of their GDP and CO_2 emissions (real and carbon economies, respectively). Multidimensional scaling and the optimal silhouette score identify $k = 2$ clusters, revealing two primary classes of countries with respect to their real and carbon economies. Notably, most countries are classified in one cluster, with only a small collection determined to belong to the second cluster. The countries in the minority cluster are Brazil, Canada, France, Germany, Italy, Mexico and the UK. This suggests that the latent factor causing separation in the lower dimensional vector space is related to GDP, rather than population. For instance, Pakistan, which has a population of *sim* 220 million people, is determined to exist in the former cluster.

We also present the hierarchical clustering results of our aggregate distance matrix across all three attributes. Figure 6 highlights the existence of one prominent cluster, a small subcluster and an outlier. The primary cluster consists

of three subclusters. The first contains countries such as Chile, Iraq, Vietnam, Romania, Bangladesh, and others. Most countries in this cluster are characterised by developing economies, growth in population, and significant growth in CO₂ emissions over time. The second subcluster consists of countries such as the Netherlands, Argentina, Nigeria, and Taiwan. These countries mostly display consistent growth in GDP and population and lower levels of CO₂ emissions over time. The final subcluster consists of Spain, South Korea, Indonesia, Mexico, Canada and Turkey. Most of these countries displayed moderate growth in GDP and population, and growth in CO₂ emissions, exhibiting reasonable variability over time. In particular, many of these countries experience a flattening in emissions over the final 5-10 years of the analysis window. The second cluster includes the UK, France, Italy and Brazil. These countries are characterised by increasing emissions trajectories until the later parts of the analysis window, where a flattening or decline in emissions occurs. Germany is identified as an outlier, which is due to its steady decline in emissions over time and the strong GDP growth over the entire analysis window. It provides a model example of successful economic growth while reducing its environmental impact.

6. Discussion

6.1. *Summary of findings*

The central focus of this paper is the evolutionary study of spatio-temporal trends in global and country-specific emission behaviours over time. In our first section, we demonstrate that most countries are well modelled by a (not necessarily continuous) piecewise linear data generating process. The consistency of this finding is surprising and would be interesting to monitor moving forward given the potential for exogenous political and social factors to alter country behaviours. Next, we demonstrate pronounced heterogeneity in cluster number, cluster size and constituency among emissions trajectories on a decade-by-decade basis. This section highlights the dynamic nature of this problem and the need for constant monitoring of country behaviours. Then, the evolutionary study of geographic variance reveals a peak in emissions' spatial dispersion in the year 2000, beyond which emissions have become more spatially concentrated. We highlight that this is largely due to China's accounting for a disproportionate level of the global emissions distribution in recent years. Finally, we introduce a framework to group countries based on their real and carbon economies. Our methodology captures emissions data, GDP and population over the past 50 years, and incorporates dimensionality reduction and clustering. This framework could be applied to other problems, or one could generalise some of the questions explored in this paper using different economic and demographic metrics.

6.2. *Limitations and future work*

There are a variety of avenues researchers could explore when considering avenues for future research. We have applied the concept of geodesic variance to country emissions trajectories. One could extend this analysis to study the

geographic spread in emissions among specific industries and identify which sectors of the economy are the most serious violators. Building upon this analysis, one could then study the “elasticity” of such emissions and build models to identify which sectors of the economy have emissions that are most easily reduced.

More broadly, given the timeliness and importance of global decarbonisation, a richer dataset with more covariates (such as industry of emissions) could allow policymakers and scientists to build more detailed models for various problems pertaining to prediction and statistical inference. Furthermore, this paper does not consider exogenous factors that may influence emissions; one could explicitly account for societal and political influences in overall emissions behaviours via random or fixed-effects models. Related to this idea, one could build a ranking system of emissions from those countries or industries that provide the most societal or economic benefit per unit omitted. One could conceivably then rank such emissions and determine which are most easily reduced and will have the smallest impact on the economy.

Appendix A. Proposition on geographic variance

Proposition Appendix A.1. *Let f be a probability density function on a finite metric space (X, d) , and consider its geodesic variance, defined by (4). That is,*

$$\text{Var}(f) = \int_{X \times X} d(x, y)^2 d\mu(x) d\mu(y) \quad (\text{A.1})$$

$$= \sum_{x, y \in X} d(x, y)^2 f(x) f(y). \quad (\text{A.2})$$

When (X, d) is a finite subset of the real number line \mathbb{R} with the Euclidean metric, this quantity reduces to the classical definition of variance, up to a factor of 2.

Proof. Let Y be a random variable on the real number line \mathbb{R} . The classical definition of variance is the quantity $\text{var}(Y) = \mathbb{E} Y^2 - (\mathbb{E} Y)^2$. If Y has a density f over a (finite) set X , this can be expressed as

$$\text{var}(Y) = \sum_{x \in X} x^2 f(x) - \left(\sum_{x \in X} x f(x) \right)^2. \quad (\text{A.3})$$

On the other hand, (A.1) can be expanded as follows:

$$\text{Var}(f) = \sum_{x,y \in X} (x - y)^2 f(x)f(y) \quad (\text{A.4})$$

$$= \sum_{x,y \in X} x^2 f(x)f(y) + \sum_{x,y \in X} y^2 f(x)f(y) - 2 \sum_{x,y \in X} xy f(x)f(y) \quad (\text{A.5})$$

$$= 2 \sum_{x,y \in X} x^2 f(x)f(y) - 2 \sum_{x,y \in X} xy f(x)f(y) \quad (\text{A.6})$$

$$= 2 \sum_{x \in X} x^2 f(x) - 2 \left(\sum_{x \in X} x f(x) \right) \left(\sum_{y \in X} y f(y) \right) \quad (\text{A.7})$$

$$= 2\text{var}(Y). \quad (\text{A.8})$$

Thus, up to a factor of 2, the geodesic (or geographic) variance reduces to the classical notion of variance on the real line. \square

With more care, the above proposition holds if X is an arbitrary metric space, with μ, ν appropriately integrable measures on X .

References

- [1] Climate change, <https://www.who.int/heli/risks/climate/climatechange/en/>, 2022. World Health Organization.
- [2] Climate change and health, <https://www.who.int/news-room/fact-sheets/detail/climate-change-and-health>, 2021. World Health Organization, 30 October 2021.
- [3] H. V. Ribeiro, D. Rybski, J. P. Kropp, Effects of changing population or density on urban carbon dioxide emissions, *Nature Communications* 10 (2019). doi:10.1038/s41467-019-11184-y.
- [4] S. Adams, C. Nsiah, Reducing carbon dioxide emissions: Does renewable energy matter?, *Science of The Total Environment* 693 (2019) 133288. doi:10.1016/j.scitotenv.2019.07.094.
- [5] S. S. Akadiri, A. A. Alola, G. Olasehinde-Williams, M. U. Etokakpan, The role of electricity consumption, globalization and economic growth in carbon dioxide emissions and its implications for environmental sustainability targets, *Science of The Total Environment* 708 (2020) 134653. doi:10.1016/j.scitotenv.2019.134653.
- [6] D. Shindell, G. Faluvegi, K. Seltzer, C. Shindell, Quantified, localized health benefits of accelerated carbon dioxide emissions reductions, *Nature Climate Change* 8 (2018) 291–295. doi:10.1038/s41558-018-0108-y.

- [7] C. Zhou, S. Wang, J. Wang, Examining the influences of urbanization on carbon dioxide emissions in the yangtze river delta, china: Kuznets curve relationship, *Science of The Total Environment* 675 (2019) 472–482. doi:10.1016/j.scitotenv.2019.04.269.
- [8] G. Dowell, J. Niederdeppe, J. Vanucchi, T. Dogan, K. Donaghy, R. Jacobson, N. Mahowald, M. Milstein, T. J. Zelikova, Rooting carbon dioxide removal research in the social sciences, *Interface Focus* 10 (2020) 20190138. doi:10.1098/rsfs.2019.0138.
- [9] N. Nechita-Banda, M. Krol, G. R. van der Werf, J. W. Kaiser, S. Pandey, V. Huijnen, C. Clerbaux, P. Coheur, M. N. Deeter, T. Röckmann, Monitoring emissions from the 2015 indonesian fires using CO satellite data, *Philosophical Transactions of the Royal Society B: Biological Sciences* 373 (2018) 20170307. doi:10.1098/rstb.2017.0307.
- [10] A. C. Serrenho, J. B. Norman, J. M. Allwood, The impact of reducing car weight on global emissions: the future fleet in great britain, *Philosophical Transactions of the Royal Society A: Mathematical, Physical and Engineering Sciences* 375 (2017) 20160364. doi:10.1098/rsta.2016.0364.
- [11] N. H. A. Bowerman, D. J. Frame, C. Huntingford, J. A. Lowe, M. R. Allen, Cumulative carbon emissions, emissions floors and short-term rates of warming: implications for policy, *Philosophical Transactions of the Royal Society A: Mathematical, Physical and Engineering Sciences* 369 (2011) 45–66. doi:10.1098/rsta.2010.0288.
- [12] M. Wang, C. Feng, Decoupling economic growth from carbon dioxide emissions in china's metal industrial sectors: A technological and efficiency perspective, *Science of The Total Environment* 691 (2019) 1173–1181. doi:10.1016/j.scitotenv.2019.07.190.
- [13] S. Naz, R. Sultan, K. Zaman, A. M. Aldakhil, A. A. Nassani, M. M. Q. Abro, Moderating and mediating role of renewable energy consumption, FDI inflows, and economic growth on carbon dioxide emissions: evidence from robust least square estimator, *Environmental Science and Pollution Research* 26 (2018) 2806–2819. doi:10.1007/s11356-018-3837-6.
- [14] T. Tong, J. Ortiz, C. Xu, F. Li, Economic growth, energy consumption, and carbon dioxide emissions in the e7 countries: a bootstrap ARDL bound test, *Energy, Sustainability and Society* 10 (2020). doi:10.1186/s13705-020-00253-6.
- [15] F. V. Bekun, F. Emir, S. A. Sarkodie, Another look at the relationship between energy consumption, carbon dioxide emissions, and economic growth in south africa, *Science of The Total Environment* 655 (2019) 759–765. doi:10.1016/j.scitotenv.2018.11.271.

- [16] Z. Liu, P. Jiang, J. Wang, L. Zhang, Ensemble system for short term carbon dioxide emissions forecasting based on multi-objective tangent search algorithm, *Journal of Environmental Management* 302 (2022) 113951. doi:10.1016/j.jenvman.2021.113951.
- [17] K. Mason, J. Duggan, E. Howley, Forecasting energy demand, wind generation and carbon dioxide emissions in ireland using evolutionary neural networks, *Energy* 155 (2018) 705–720. doi:10.1016/j.energy.2018.04.192.
- [18] P. Sutthichaimethee, D. Ariyasajjakorn, Forecast of carbon dioxide emissions from energy consumption in industry sectors in thailand, *Environmental and Climate Technologies* 22 (2018) 107–117. doi:10.2478/rtuect-2018-0007.
- [19] Y.-J. Chiu, Y.-C. Hu, P. Jiang, J. Xie, Y.-W. Ken, A multivariate grey prediction model using neural networks with application to carbon dioxide emissions forecasting, *Mathematical Problems in Engineering* 2020 (2020) 1–10. doi:10.1155/2020/8829948.
- [20] D. Töbelmann, T. Wendler, The impact of environmental innovation on carbon dioxide emissions, *Journal of Cleaner Production* 244 (2020) 118787. doi:10.1016/j.jclepro.2019.118787.
- [21] G. P. Peters, R. M. Andrew, J. G. Canadell, P. Friedlingstein, R. B. Jackson, J. I. Korsbakken, C. L. Quéré, A. Pregon, Carbon dioxide emissions continue to grow amidst slowly emerging climate policies, *Nature Climate Change* 10 (2019) 3–6. doi:10.1038/s41558-019-0659-6.
- [22] S. Holloway, Carbon dioxide capture and geological storage, *Philosophical Transactions of the Royal Society A: Mathematical, Physical and Engineering Sciences* 365 (2007) 1095–1107. doi:10.1098/rsta.2006.1953.
- [23] T. J. Zelikova, The future of carbon dioxide removal must be transdisciplinary, *Interface Focus* 10 (2020) 20200038. doi:10.1098/rsfs.2020.0038.
- [24] C. Gao, H. Ge, Spatiotemporal characteristics of china’s carbon emissions and driving forces: A five-year plan perspective from 2001 to 2015, *Journal of Cleaner Production* 248 (2020) 119280. doi:10.1016/j.jclepro.2019.119280.
- [25] M. Hu, R. Li, W. You, Y. Liu, C.-C. Lee, Spatiotemporal evolution of decoupling and driving forces of CO₂ emissions on economic growth along the belt and road, *Journal of Cleaner Production* 277 (2020) 123272. doi:10.1016/j.jclepro.2020.123272.
- [26] A. Roobaert, G. G. Laruelle, P. Landschützer, N. Gruber, L. Chou, P. Rignier, The spatiotemporal dynamics of the sources and sinks of CO₂ in the global coastal ocean, *Global Biogeochemical Cycles* 33 (2019) 1693–1714. doi:10.1029/2019gb006239.

- [27] N. James, M. Menzies, H. Bondell, Comparing the dynamics of COVID-19 infection and mortality in the United States, India, and Brazil, *Physica D: Nonlinear Phenomena* 432 (2022) 133158. doi:10.1016/j.physd.2022.133158.
- [28] G. Chowell, L. Sattenspiel, S. Bansal, C. Viboud, Mathematical models to characterize early epidemic growth: A review, *Physics of Life Reviews* 18 (2016) 66–97. doi:10.1016/j.plrev.2016.07.005.
- [29] C. Manchein, E. L. Brugnago, R. M. da Silva, C. F. O. Mendes, M. W. Beims, Strong correlations between power-law growth of COVID-19 in four continents and the inefficiency of soft quarantine strategies, *Chaos: An Interdisciplinary Journal of Nonlinear Science* 30 (2020) 041102. doi:10.1063/5.0009454.
- [30] N. James, M. Menzies, Estimating a continuously varying offset between multivariate time series with application to COVID-19 in the United States, *The European Physical Journal Special Topics* (2022). doi:10.1140/epjs/s11734-022-00430-y.
- [31] B. Blasius, Power-law distribution in the number of confirmed COVID-19 cases, *Chaos: An Interdisciplinary Journal of Nonlinear Science* 30 (2020) 093123. doi:10.1063/5.0013031.
- [32] N. James, M. Menzies, Trends in COVID-19 prevalence and mortality: A year in review, *Physica D: Nonlinear Phenomena* 425 (2021) 132968. doi:10.1016/j.physd.2021.132968.
- [33] A. Prakash, N. James, M. Menzies, G. Francis, Structural clustering of volatility regimes for dynamic trading strategies, *Applied Mathematical Finance* (2022) 1–39. doi:10.1080/1350486X.2021.2007146.
- [34] S. Drożdż, J. Kwapien, P. Oświęcimka, T. Stanisz, M. Wątorek, Complexity in economic and social systems: Cryptocurrency market at around COVID-19, *Entropy* 22 (2020) 1043. doi:10.3390/e22091043.
- [35] N. James, M. Menzies, Association between COVID-19 cases and international equity indices, *Physica D: Nonlinear Phenomena* 417 (2021) 132809. doi:10.1016/j.physd.2020.132809.
- [36] S. Drożdż, J. Kwapien, P. Oświęcimka, Complexity in economic and social systems, *Entropy* 23 (2021) 133. doi:10.3390/e23020133.
- [37] N. James, M. Menzies, Efficiency of communities and financial markets during the 2020 pandemic, *Chaos: An Interdisciplinary Journal of Nonlinear Science* 31 (2021) 083116. doi:10.1063/5.0054493.
- [38] N. James, M. Menzies, Collective correlations, dynamics, and behavioural inconsistencies of the cryptocurrency market over time, *Nonlinear Dynamics* (2022). doi:10.1007/s11071-021-07166-9.

- [39] A. Vazquez, Polynomial growth in branching processes with diverging reproductive number, *Physical Review Letters* 96 (2006). doi:10.1103/physrevlett.96.038702.
- [40] C. F. Mendes, M. W. Beims, Distance correlation detecting Lyapunov instabilities, noise-induced escape times and mixing, *Physica A: Statistical Mechanics and its Applications* 512 (2018) 721–730. doi:10.1016/j.physa.2018.08.028.
- [41] K. Shang, B. Yang, J. M. Moore, Q. Ji, M. Small, Growing networks with communities: A distributive link model, *Chaos: An Interdisciplinary Journal of Nonlinear Science* 30 (2020) 041101. doi:10.1063/5.0007422.
- [42] N. James, M. Menzies, H. Bondell, In search of peak human athletic potential: a mathematical investigation, *Chaos: An Interdisciplinary Journal of Nonlinear Science* 32 (2022). doi:10.1063/5.0073141.
- [43] H. W. Hethcote, The mathematics of infectious diseases, *SIAM Review* 42 (2000) 599–653. doi:10.1137/s0036144500371907.
- [44] M. Perc, N. G. Miksić, M. Slavinec, A. Stožer, Forecasting COVID-19, *Frontiers in Physics* 8 (2020) 127. doi:10.3389/fphy.2020.00127.
- [45] N. James, M. Menzies, A new measure between sets of probability distributions with applications to erratic financial behavior, *Journal of Statistical Mechanics: Theory and Experiment* 2021 (2021) 123404. doi:10.1088/1742-5468/ac3d91.
- [46] R. Moeckel, B. Murray, Measuring the distance between time series, *Physica D: Nonlinear Phenomena* 102 (1997) 187–194. doi:10.1016/s0167-2789(96)00154-6.
- [47] G. J. Székely, M. L. Rizzo, N. K. Bakirov, Measuring and testing dependence by correlation of distances, *The Annals of Statistics* 35 (2007) 2769–2794. doi:10.1214/009053607000000505.
- [48] C. F. O. Mendes, R. M. da Silva, M. W. Beims, Decay of the distance autocorrelation and Lyapunov exponents, *Physical Review E* 99 (2019). doi:10.1103/physreve.99.062206.
- [49] N. James, M. Menzies, L. Azizi, J. Chan, Novel semi-metrics for multivariate change point analysis and anomaly detection, *Physica D: Nonlinear Phenomena* 412 (2020) 132636. doi:10.1016/j.physd.2020.132636.
- [50] A. Karaivanov, A social network model of COVID-19, *PLOS ONE* 15 (2020) e0240878. doi:10.1371/journal.pone.0240878.
- [51] J. Ge, D. He, Z. Lin, H. Zhu, Z. Zhuang, Four-tier response system and spatial propagation of COVID-19 in China by a network model, *Mathematical Biosciences* 330 (2020) 108484. doi:10.1016/j.mbs.2020.108484.

- [52] L. Xue, S. Jing, J. C. Miller, W. Sun, H. Li, J. G. Estrada-Franco, J. M. Hyman, H. Zhu, A data-driven network model for the emerging COVID-19 epidemics in Wuhan, Toronto and Italy, *Mathematical Biosciences* 326 (2020) 108391. doi:10.1016/j.mbs.2020.108391.
- [53] J. A. T. Machado, A. M. Lopes, Rare and extreme events: the case of COVID-19 pandemic, *Nonlinear Dynamics* (2020). doi:10.1007/s11071-020-05680-w.
- [54] C. N. Ngonghala, E. A. Iboi, A. B. Gumel, Could masks curtail the post-lockdown resurgence of COVID-19 in the US?, *Mathematical Biosciences* 329 (2020) 108452. doi:10.1016/j.mbs.2020.108452.
- [55] J. Cavataio, S. Schnell, Interpreting SARS-CoV-2 seroprevalence, deaths, and fatality rate — making a case for standardized reporting to improve communication, *Mathematical Biosciences* 333 (2021) 108545. doi:10.1016/j.mbs.2021.108545.
- [56] L. Ó. Náraigh, Á. Byrne, Piecewise-constant optimal control strategies for controlling the outbreak of COVID-19 in the Irish population, *Mathematical Biosciences* 330 (2020) 108496. doi:10.1016/j.mbs.2020.108496.
- [57] D. H. Glass, European and US lockdowns and second waves during the COVID-19 pandemic, *Mathematical Biosciences* 330 (2020) 108472. doi:10.1016/j.mbs.2020.108472.
- [58] N. James, M. Menzies, H. Bondell, Understanding spatial propagation using metric geometry with application to the spread of COVID-19 in the United States, *EPL (Europhysics Letters)* 135 (2021) 48004. doi:10.1209/0295-5075/ac2752.
- [59] G. V. Brummelen, *Heavenly Mathematics: The Forgotten Art of Spherical Trigonometry*, Princeton University Press, 2013.
- [60] P. J. Rousseeuw, *Silhouettes: A graphical aid to the interpretation and validation of cluster analysis*, *Journal of Computational and Applied Mathematics* 20 (1987) 53–65. doi:10.1016/0377-0427(87)90125-7.